Applied Mathematics and Computation 217 (2010) 1704–1718

Contents lists available at ScienceDirect

Applied Mathematics and Computation

journal homepage: www.elsevier.com/locate/amc

Solitary wave transformation on the underwater step: Asymptotic theory and numerical experiments

Efim Pelinovsky [a,b,*], Byung Ho Choi [c], Tatiana Talipova [a], Seung Buhm Woo [d], Dong Chule Kim [c]

[a] Department of Nonlinear Geophysical Processes, Institute of Applied Physics, Nizhny Novgorod, Russia
[b] Department of Mathematical Sciences, Loughborough University, Loughborough, UK
[c] Department of Civil and Environmental Engineering, Sungkyuankwan University, Suwon, Republic of Korea
[d] Department of Oceanography, Inha University, Inchon, Republic of Korea

ARTICLE INFO

Keywords:
Korteweg–de Vries equation
Boussinesq system
Navier–Stokes equations
Water waves
Ideal and viscous fluid
Numerical modelling
FLOW3D
CADMAS

ABSTRACT

The transformation of a solitary wave on an underwater step is studied analytically and numerically. The theoretical model includes the linear potential description of the wave transformation on a step and the weakly nonlinear theory of long waves based on the Korteweg–de Vries equation for reflected and transmitted waves far from a step. Numerical simulation of solitary wave transformation on an underwater step is performed in the framework of an extended 1D Boussinesq-like system and fully nonlinear fully dispersive 2D Navier–Stokes equations. The results of numerical simulations for the incident solitary wave of weak amplitude are in agreement with the theoretical predictions for the wave shapes of the secondary solitons, but not with the predictions for travel times.

© 2009 Elsevier Inc. All rights reserved.

1. Introduction

The Korteweg–de Vries soliton transformation in a shallow fluid above a gentle beach has been studied by [1–3]. The transition zone of variable depth induces, in general, soliton fission into a train of solitons plus an oscillatory tail. If the depth is varied very smoothly (characteristic length is bigger than nonlinear and dispersive scales), the solitary wave remains the soliton in main order of perturbation theory ($A \sim h^{-1}$, where A is the soliton amplitude and h is water depth), and only the oscillatory tail is formed [4]. If the depth is varied smoothly (in the sense of the linear WKB approximation that the characteristic length of depth variation is bigger than the soliton length but smaller than nonlinear and dispersive scales), the soliton transformation in the gradient region between two uniform regions is described by the "linear" Green law $A \sim h^{-1/4}$, and its shape is described by the sech^2-function. It is possible to obtain the explicit formulas for the secondary solitons formed in the transmitted wave, and this case has been analyzed in [1–3]. The same processes have been described theoretically for internal waves in a stratified fluid [5,6], where the situation is more complicated for certain conditions in which the sign of the nonlinear coefficient can change, leading to the appearance of secondary solitons of opposite polarity [7–9]. The features of the soliton fission process in the periodic variable-coefficient Korteweg–de Vries equation are studied in [10].

Similar processes can be investigated for solitons in rapidly varied media, and some theoretical results are given in [2,11–16]. With applications to water waves, the description of long wave transformation at an underwater step is the key problem in wave scattering theory. In the theoretical plane, even within the linear Euler equations this problem has no simple analytical solution. Physically, it is evident that in the vicinity of the step, the long wave approximation breaks due to strong vertical motion of water particles. Mathematically, the long wave solution does not formally satisfy the exact boundary

* Corresponding author. Address: Department of Nonlinear Geophysical Processes, Institute of Applied Physics, Nizhny Novgorod, Russia.
E-mail address: Pelinovsky@hydro.appl.sci-nnov.ru (E. Pelinovsky).

0096-3003/$ - see front matter © 2009 Elsevier Inc. All rights reserved.
doi:10.1016/j.amc.2009.10.029

condition at a step (no penetration through the vertical wall), and many truncated (non-propagated) modes are generated in the vicinity of a step; see for instance [17]. Such modes are important only in the vicinity of a step, and their amplitudes are reduced exponentially with distance from the step. They do not influence the energy flux far from the step [17]. This limitation of influence was first shown rigorously in the framework of the linear potential theory of water waves in the pioneer paper by [18]. The exact linear potential model confirms the prediction of the linear shallow-water model for amplitudes of the reflected and transmitted waves if the incident wave is a long one.

Generally speaking, nonlinearity of the wave field changes the wave characteristics at a step. Using nonlinear shallow water theory for a long wave passing over a step, [19] showed that nonlinear effects are relatively weak if the wave amplitude does not exceed the water depth. [20] developed an edge-layer theory taking into account both nonlinear and dispersive effects for small-amplitude soliton transformation over a step, and showed that the formulas of the linear shallow-water theory can give correct results for wave amplitudes in the vicinity of a step. Far from the step, the transmitted and reflected waves transform due to both nonlinear and dispersive effects; this scenario is in fact the same as the one pointed out in the previous paragraph.

Surface wave transformation through a step has been studied experimentally [21,22] and numerically [21–24]. Two numerical models have been used to simulate this process: 1D Curvature Effects Including Long Wave (CEILW) equations [21] and 2D Reynolds Averaged Navier–Stokes (RANS) equations [22–24]. Laboratory and numerical RANS modeling has shown the complicated flow dynamics in the vicinity of a step, including vortex generation due to flow separation at the corners of the obstacle. Meanwhile, on average, the characteristics of the transmitted and reflected waves computed in the framework of potential and viscous fluid are in good agreement with laboratory data. If the soliton amplitude is weak, the results of laboratory and numeric experiments are close to the predictions of soliton amplitudes formed in reflected and transmitted waves given by the framework of weakly-nonlinear theory [2,12,20].

The goal of this paper is to continue the study of solitary wave transformation above the bottom step, by performing two tasks: (i) to investigate the applicability of the asymptotic theory based on the Korteweg–de Vries equation to describe the wave process on all stages of wave transformation and fission, (ii) to study this process numerically using several 1D and 2D models of ideal and viscous fluid. Numerical simulation is performed in the framework of various hydrodynamic nonlinear-dispersive models: two versions of the extended Boussinesq-like systems and two versions of the Reynolds-averaged Navier–Stokes equations, all of them well validated on laboratory data. An analytical approximated solution has been obtained by matching the linear shallow-water theory in the vicinity of a step with the weakly nonlinear-dispersive theory for waves far from a step; it was published originally in Russian and French [2,11], and then reproduced in [21]. In Section 2, this solution is briefly described. Detailed characteristics of the process of soliton fission in the reflected and transmitted wave fields are investigated in the framework of the Korteweg–de Vries equation (Section 3). Solitary wave transformation on a step is computed in the framework of various nonlinear-dispersive models: 1D Boussinesq-like systems and 2D Reynolds Averaged Navier–Stokes equations; in total, four numerical codes are used (Section 4). A comparison of the results obtained in the framework of the various models is presented in Section 5. In general, the amplitudes of the secondary solitons in the transmitted wave field are the same in the framework of various models and coincide with theoretical predictions; this conclusion is in agreement with the numerical and laboratory results given in [21–24]. The travel times of energetic waves are different in various models, and the Korteweg–de Vries model overestimates them. The obtained results are summarized in the conclusion.

2. Analytical theory of solitary wave transformation at a step

Let us describe briefly the analytical theory of solitary wave (soliton) transformation at a bottom step (Fig. 1), developed in [2,12]. It is based on a two-step approach: the linear shallow-water theory in the vicinity of a step and the Korteweg–de Vries equation for the wave field far from the step. According to the linear shallow-water theory, the amplitudes (heights) of transmitted (H_{tr}) and reflected (H_r) waves at a step are described by well-known formulas (see for instance, [17,25]).

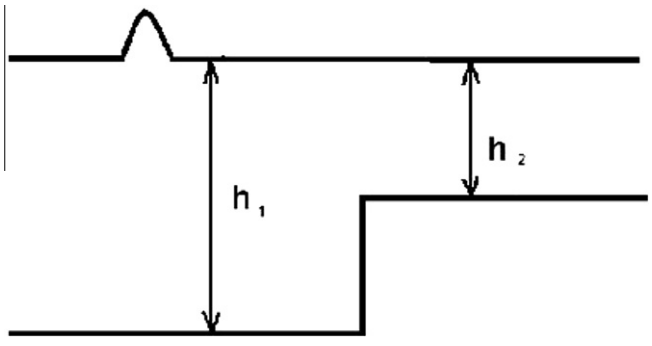


Fig. 1. Problem geometry.

$$\frac{H_{tr}}{H_0}=\frac{2}{1+\sqrt{h_2/h_1}},\quad \frac{H_r}{H_0}=\frac{1-\sqrt{h_2/h_1}}{1+\sqrt{h_2/h_1}}, \tag{1}$$

where H_0 is the amplitude of the incident wave. The wave shape is not changed in the framework of the linear shallow-water theory.

It is important to note that transmission and reflection coefficients are positive, and therefore, the polarity of the transmitted and reflected waves is the same as that of the incident wave (for wave passage from deep to shallow water). Also, it is important to mention that the wave duration is not changed when the wave passes through a step, but the length of the transmitted wave is changed accordingly to

$$\frac{\lambda_{tr}}{\lambda_0}=\sqrt{\frac{h_2}{h_1}},\quad \lambda_r=\lambda_0, \tag{2}$$

where λ_0 is the incident wavelength.

The solution described above is obtained in the framework of the linear shallow-water theory; see for instance [17,25]. Formally, it does not satisfy the exact boundary condition at a step in the frame of initial Euler equations (zero horizontal velocity on the wall), as was mentioned in Section 1. Taking into account the fluid viscosity, vortices formed due to flow separation at the step [22]. Meanwhile, [20] developed an edge-layer theory for small-amplitude soliton transformation over a step and showed that Eq. (1) "can still give correct information so far as the amplitudes are concerned". The same result was then obtained in numerical studies, for numerical results given in [24] "agree excellently with" Eq. (1). This agreement means that we may use the linear shallow-water theory to describe the wave transformation over a step for both linear and weakly nonlinear waves. However, weakly nonlinear and dispersive effects may be important in the next stage of wave evolution far from a step in both directions.

Far from a step, a weakly nonlinear-dispersive theory can be applied to describe wave characteristics. Its simplest variant is based on the famous Korteweg–de Vries equation

$$\frac{\partial\eta}{\partial t}+c\left(1+\frac{3\eta}{2h}\right)\frac{\partial\eta}{\partial x}+\frac{ch^2}{6}\frac{\partial^3\eta}{\partial x^3}=0, \tag{3}$$

which should be solved independently for reflected and transmitted waves (axis x will be directed from the step for each wave). This equation is fully integrable mathematically and has been extensively studied (see, for instance, [26]). The main result here is that a pulse-like disturbance does not conserve its shape (except for a single soliton) and evolves in general into solitons and dispersive wave packets; such transformation explains the appearance of secondary soliton-like waves and undular bores in shallow water [27–29], and in particular the ones observed during the last huge tsunami in the Indian Ocean in 2004 [30,31]. The characteristic scales of the nonlinear-dispersive wave transformation are the nonlinear length-scale, L_{nl} and the dispersive length-scale, L_{dis}, [13,28,32]

$$L_{nl}\sim\lambda(h/H),\quad L_{dis}\sim\lambda^3/h^2. \tag{4}$$

The solitary wave (soliton) solution of the Korteweg–de Vries Eq. (3) is well known:

$$\eta(x,t)=H\mathrm{sech}^2\left[\sqrt{\frac{3H}{4h}}\frac{x-c(1+3H/2h)t}{h}\right],\quad \lambda=2h\sqrt{\frac{h}{H}}, \tag{5}$$

2.1. where λ is the characteristic wavelength of the solitary wave at the 0.5-level

We assume that the incident solitary wave has a soliton-like shape (5) with H_0, h_1 and c_1. Such a wave propagates to the step with no changes in its shape and amplitude. At a step, due to weak nonlinearity and dispersion, the process of the wave transformation in the vicinity of a step can be described in the framework of linear shallow-water theory (1) and (2). After the transformation at a step, the transmitted and reflected waves are

$$\eta_{tr}(t)=\frac{2H_0}{1+\sqrt{h_2/h_1}}\mathrm{sech}\,h^2\left[\sqrt{\frac{3gH_0}{4h_1^2}}t\right], \tag{6}$$

$$\eta_r(t)=H_0\frac{1-\sqrt{h_2/h_1}}{1+\sqrt{h_2/h_1}}\mathrm{sech}^2\left[\sqrt{\frac{3gH_0}{4h_1^2}}t\right]. \tag{7}$$

Both waves have soliton-like shapes at a step, but they are not steady-state solitons because their lengths and amplitudes do not satisfy Eq. (5). As a result, according to the rigorous mathematical theory of the Korteweg–de Vries equation [26], they will evolve into solitons and dispersive trains. In this case the functions (6) and (7) can be used as initial conditions for the Korteweg–de Vries equation for each wave. Because the wave propagates from a step, it is convenient to re-write the Korteweg–de Vries equation (3) in equivalent form

$$\frac{\partial\eta}{\partial x}-\frac{3\eta}{2hc}\frac{\partial\eta}{\partial\tau}-\frac{h^2}{6c^3}\frac{\partial^3\eta}{\partial\tau^3}=0,\quad \tau=t-\frac{x}{c}, \tag{8}$$

which has the same accuracy as (3) due to weak nonlinearity and dispersion [28,33]. So, Eq. (8) must be solved, with adequate "initial" conditions (6) and (7) at $x = 0$, independently for $x > 0$ and for $x < 0$. The time in (8) should be shifted on travel time from the initial point to the step location. Analytical results in the framework of the Korteweg–de Vries equation can be found for instance in the book [26]. They are used to calculate the amplitudes of the secondary solitons that appear in the transmitted and reflected waves [2,12,21,13].

In particular, the amplitudes of the secondary solitons that appear in the transmitted waves are

$$\frac{A_{n+1}^{tr}}{H_0} = \frac{1}{4}\left(\frac{h_2}{h_1}\right)^2 \left[\sqrt{1 + \frac{16}{(1+\sqrt{h_2/h_1})}\left(\frac{h_2}{h_1}\right)^{-2}} - (1+2n)\right]^2, \tag{9}$$

where $n = 0, 1, \ldots, N-1$, and N is the number of secondary solitons

$$N = E\left[\frac{\sqrt{1 + \frac{16}{(1+\sqrt{h_2/h_1})}\left(\frac{h_2}{h_1}\right)^{-2}} - 1}{2}\right]. \tag{10}$$

Here $E(z)$ is the integer symbol.

In the reflected wave only one soliton appears, and its amplitude is

$$\frac{A_1^r}{H_0} = 0.25\left[\sqrt{1 + 8\frac{1-\sqrt{h_2/h_1}}{1+\sqrt{h_2/h_1}}} - 1\right]^2. \tag{11}$$

The formation of the solitons in transmitted and reflected waves is accompanied by generation of the dispersive wave train with decreased amplitude. The detailed structure of the wave field can be found numerically in the framework of the Korteweg–de Vries equation; see next section.

3. Modeling of the fission of a solitary wave passed through a step: Korteweg–de Vries equation framework

Modeling of transmitted and reflected waves is performed in the framework of the dimensionless Korteweg–de Vries equation (8) where the following normalization is used

$$\zeta = \frac{\eta}{h}, \quad \tilde{x} = \frac{x}{h}, \quad \tilde{\tau} = \sqrt{\frac{g}{h}}\tau, \tag{12}$$

and h is h_1 for the reflected wave and h_2 for the transmitted wave. The output of this model gives the time series of water displacement at various points outside a step. Due to weak nonlinearity and dispersion, computed time series can be recalculated in spatial distributions of the wave field using the linear relation: $x = ct$. The numerical scheme used here is the finite-difference scheme [34] with periodic boundary conditions

$$\zeta(t + T_p, x) = \zeta(t, x), \tag{13}$$

where T_p is the length of the computed domain, and the Courant stability criterion is applied. The domain length is 1000; the number of points equals 10000; the spatial step is less than Courant critical one and equals 0.002. In experiments the step depth ratio (h_2/h_1) is varied from 0.1 to 0.9, and the initial solitary wave amplitude H_0/h_1 is varied from 0.1 to 0.5. In fact, the high-frequency dispersive tail formed in the process of soliton fission moves quickly to the left boundary and is damped artificially there.

The evolution of the transmitted wave is shown in Fig. 2 for $h_2/h_1 = 0.5$ and an initial solitary wave amplitude $H_0/h_1 = 0.1$. Only three solitary waves are generated from the initial soliton for a given step height, according to the theory described in Section 2, and our numerical simulations confirm this.

If the depth difference is large, the number of secondary solitons also increases significantly; see Fig. 3 for $h_2/h_1 = 0.1$. The number of secondary solitons predicted by the theory is 17, and almost all of them are visible at time 600.

The reflected wave has smaller amplitudes than the transmitted wave, and more time is required for secondary soliton generation. According to the theory, only one soliton is formed in the reflected wave, see Fig. 4 for $H_0/h_1 = 0.4$ and $h_2/h_1 = 0.5$ (time 6000).

With decreasing ratio h_2/h_1, the time of secondary soliton generation is decreased. Fig. 5 demonstrates the formation of the secondary soliton in the reflected wave for parameters $H_0/h_1 = 0.1$ and $h_2/h_1 = 0.1$ at time 2000. Soliton formation requires less time than for the case described by Fig. 4, and its amplitude is bigger instead of the initial soliton amplitude is 4 times less that in previous case.

Computed values of the secondary solitons are shown as dots in Fig. 6 for the transmitted wave and in Fig. 7 for the reflected wave. The theoretical curves calculated from (9) and (11) in the framework of exact solution of the Korteweg–de Vries equation are presented also. Theoretical and computed values, as expected, are in excellent agreement.

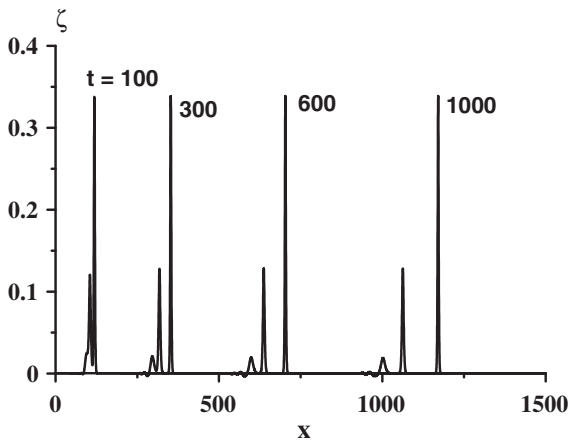


Fig. 2. Secondary solitary wave generating in the transmitted wave. Initial soliton amplitude $H_0/h_1 = 0.1$ and depth ratio $h_2/h_1 = 0.5$.

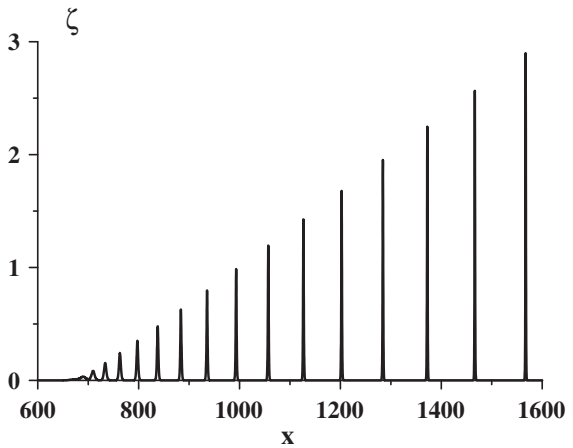


Fig. 3. Secondary solitons generated the transmitted wave for initial solution amplitude $H_0/h_1 = 0.1$ and depth ratio $h_2/h_1 = 0.1$ (time 600).

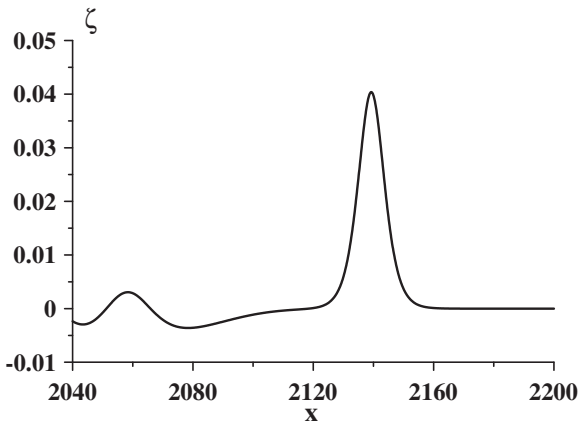


Fig. 4. Secondary soliton generated in reflected wave for $h_2/h_1 = 0.5$ and $H_0/h_1 = 0.4$ at times 6000.

For comparison of results of all models, the runs of the Korteweg–de Vries model were done in dimension form (8) with $h_1 = 10$ m, $h_2 = 5$ m, initial wave amplitude $H_0 = 0.3$ m. Both domain sizes for reflected and transmitted wave were 4000 m.

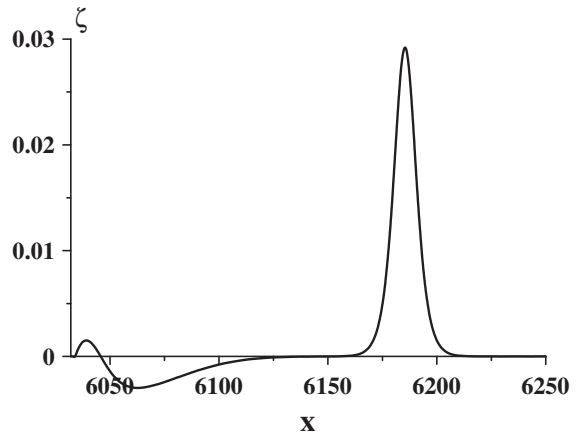


Fig. 5. Secondary soliton in reflected wave for $h_2/h_1 = 0.5$ and $H_0/h_1 = 0.4$ at time 6000 for $h_2/h_1 = 0.1$ and $H_0/h_1 = 0.1$ at time 2000.

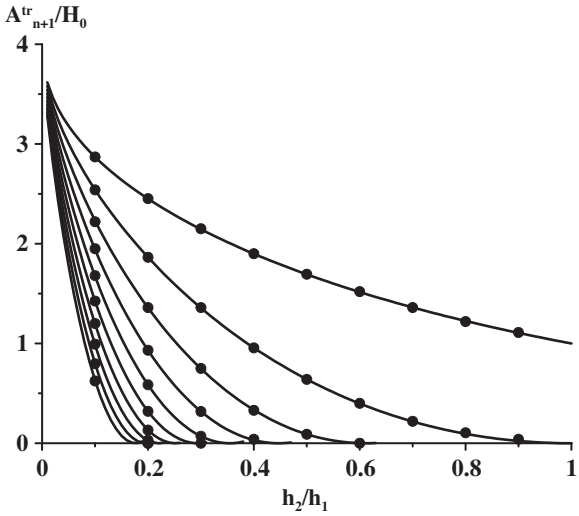


Fig. 6. Amplitudes of secondary solitons generated in the transmitted wave. Solid lines are theoretical values according to (9) and points are computed values.

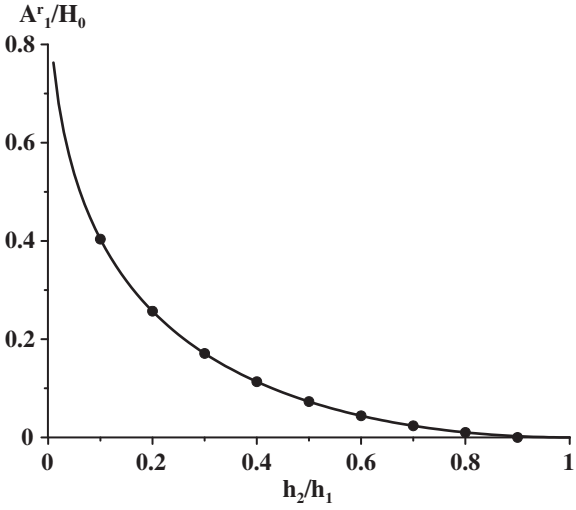


Fig. 7. Amplitude of secondary single soliton generated in reflected wave. Solid line is the theoretical values according to (11) and points are computed values.

4. Soliton fission on a step: Boussinesq-like and Navier–Stokes models

The conventional Korteweg–de Vries equation is derived only for unidirectional waves, so it can be used to study the dynamics of the transmitted and reflected waves, but not a solitary wave transformation at a step. To describe this process, it is necessary to use at least bi-directional models.

Assuming that both the nonlinearity and the frequency dispersion are weak and are of the same order of magnitude, [35] derived the Boussinesq equations for a wave field (water displacement and depth-averaged velocity) in a basin with variable depth. This model is called the "standard" Boussinesq system. The applicability of the standard Boussinesq equations is limited due to its weak dispersion, i.e., the theory cannot tell the correct wave celerity when the depth is less than one-fifth of

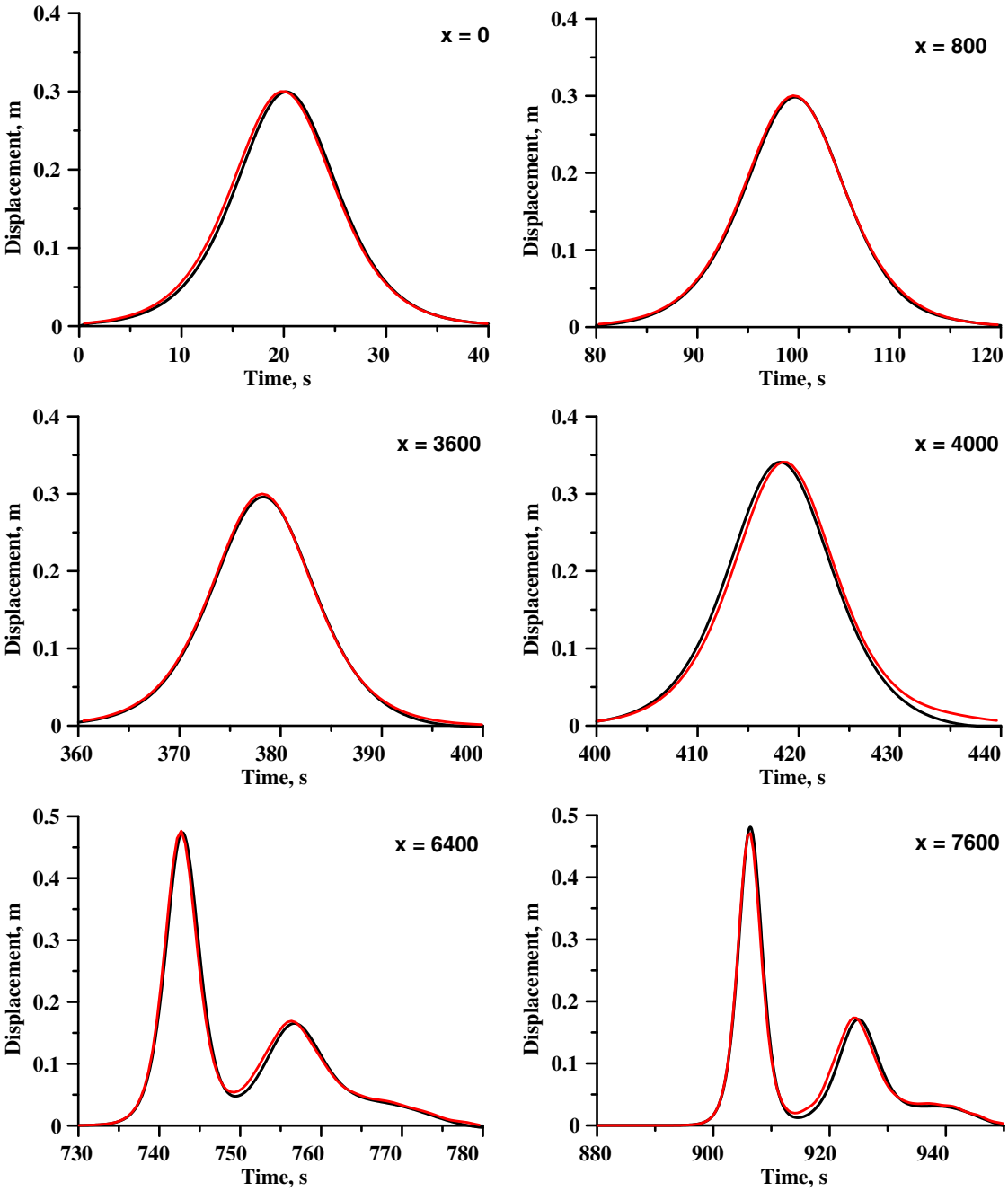


Fig. 8. Computed wave shape within two Boussinesq-like models. Black line is MIKE21 and grey line is EB_FEM.

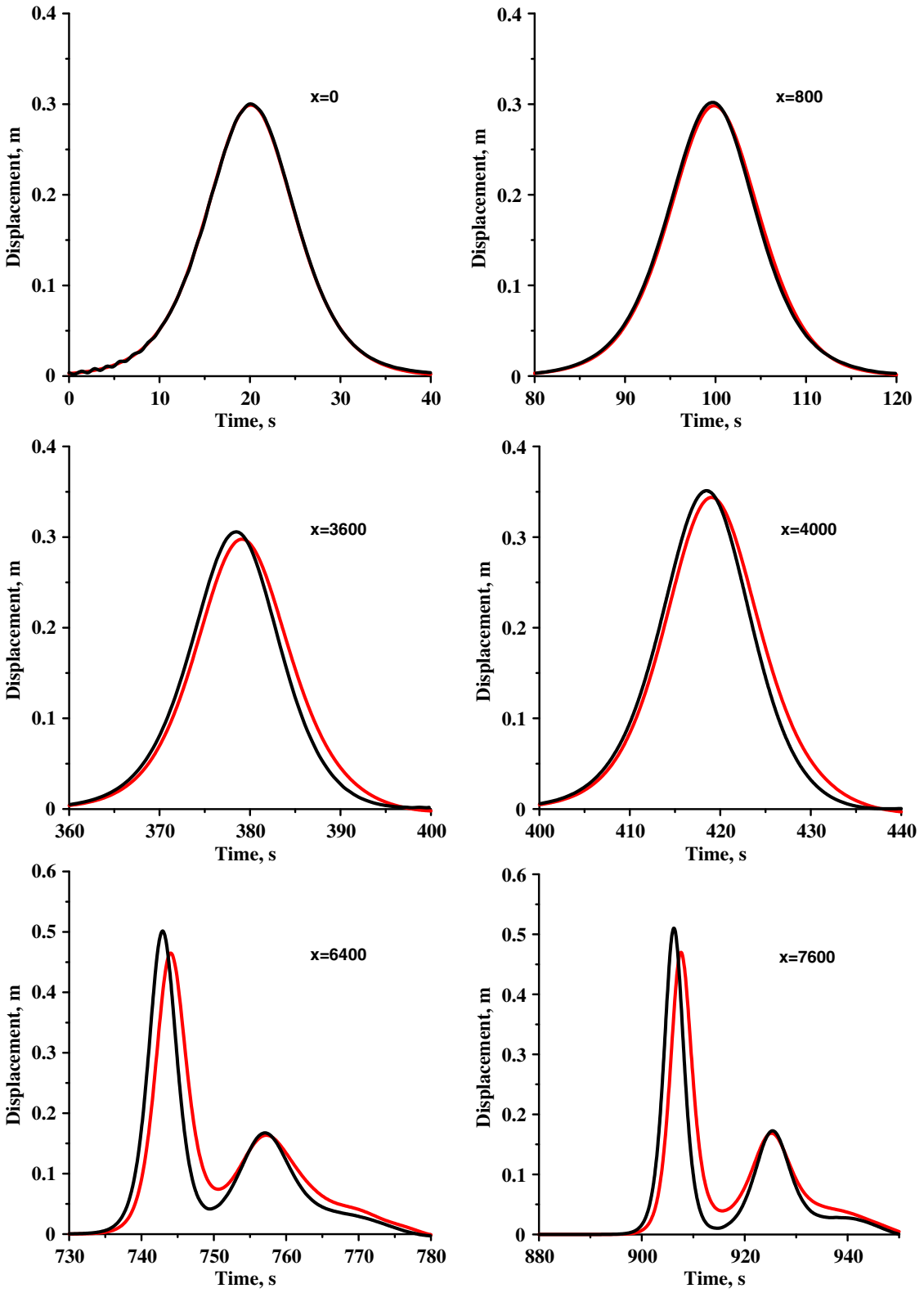


Fig. 9. The comparison of two RANS models. Black line is CADMAS and grey line is FLOW3D.

the equivalent deep-water wavelength. Furthermore, when the Boussinesq equations are solved numerically, high-frequency oscillations with wavelengths related to the grid size could cause numerical instability.

To extend the theoretical model to shorter waves, many modified forms of Boussinesq-type equations have been derived (e.g. [36–40]). This extension is related to the best fit of the exact dispersion relationship for linear water waves by polynomial approximations. In the given study, two Boussinesq-like models are applied to solitary wave transformation on a step: EB-FEM [41], and MIKE21 [38]. In particular, the basic equations of EB-FEM are

$$\frac{\partial u}{\partial t} + u\frac{\partial u}{\partial x} + g\frac{\partial \eta}{\partial x} + \frac{\theta^2 h^2}{2}\frac{\partial^2(\partial u/\partial t)}{\partial x^2} + \theta h \frac{\partial^2}{\partial x^2}\left(h\frac{\partial u}{\partial t}\right) = 0, \tag{14}$$

$$\frac{\partial \eta}{\partial t} + \frac{\partial}{\partial x}[(h+\eta)u] + \frac{\partial}{\partial x}\left(\left[\frac{\theta^2}{2} - \frac{1}{6}\right]h^3\frac{\partial^2 u}{\partial x^2} + \left[\theta + \frac{1}{2}\right]h^2\frac{\partial^2(hu)}{\partial x^2}\right) = 0 \tag{15}$$

where $u(x,t)$ is the particle velocity at fixed depth $z = \theta h$. In our computations, the parameter θ is chosen to be 0.45, meaning that the water velocity in almost middle layer is treated as representative of the depth-averaged velocity. By choosing the value of θ this way, we can greatly improve the dispersion relationship [36].

The difference between the MIKE21 and EB-FEM models is the mathematical description for frequency dispersion terms, which contains the 3rd order spatial derivative terms. The numerical schemes are also different: the EB-FEM model adopted the finite-element method, while the finite-difference scheme is used in MIKE21. Meanwhile, both models have been proved to accurately simulate deep-water wave propagation and nonlinear wave–wave interactions [38,41].

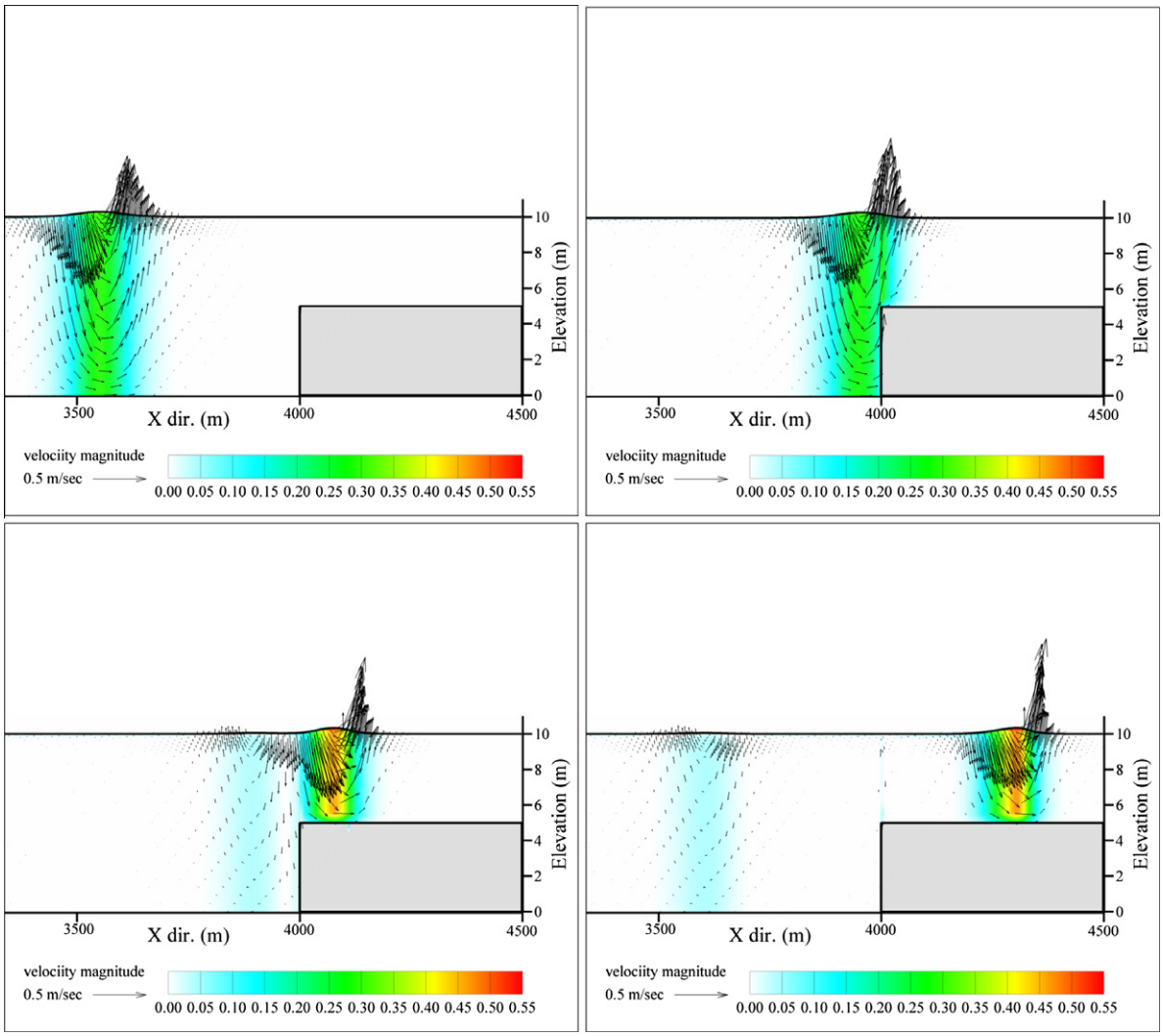


Fig. 10. Particle velocity structure computed with FLOW3D for times 105 s, 145 s, 160 s and 190 s.

It is important to mention that the Boussinesq-like models are derived for smooth-bottom topography, where the order of magnitude of the spatial depth gradient is assumed to be equal to or less than 1. For the numerical simulation in this study, however, the bathymetry has an infinite gradient at the discontinuous step. Therefore the "step bathymetry" is smoothed in computation by numerical dissipative techniques, and the detailed numerical treatment can be found in the literature [38,41].

Results of numerical simulations of solitary wave transformation on a step in the framework of these Boussinesq models are displayed in Fig. 8. In these experiments the bottom step is $h_2/h_1 = 1/2$, and the soliton amplitude is 0.3 m (initial depth $h_1 = 10$ m). Both models show very similar results.

Boussinesq-like models include only the horizontal coordinates, and the vertical momentum of the wave flow is described through the dispersion terms. In other words, the vertical flow structure is not solved directly in Boussinesq-like models, but the effect of the vertical momentum is considered through dispersion terms. In this process the vertical distribution of the particle velocity is assumed to be a polynomial increase from the bottom to the surface.

In the vicinity of the step, the vertical motion is prevailed as indicated above. In order to investigate the effect of vertical momentum in the vicinity of the step, we attempted to apply the direct simulation of Navier–Stokes equations, where no restrictions are made for vertical momentum. In our study the Reynolds-Averaged Navier–Stokes (RANS) equations are applied. An updated version of the $k-\varepsilon$ model with the help of renormalization group analysis is used to describe of turbulence [42,43]. In this study, two RANS models are applied: FLOW3D [44] and CADMAS-SURF [45]. The computational fluid dynamics code FLOW3D solves the Navier–Stokes equation by the finite difference method. It utilizes a true volume of fluid (VOF) method for computing free surface motion and the fractional area/volume obstacle representation (FAVOR) technique to model complex geometric regions. The code FLOW3D has been applied to simulate tsunami wave runup [46,47].

The CADMAS-SURF program using the VOF method solves the Navier–Stokes equations for an incompressible fluid [45]. CADMAS-SURF is different from FLOW3D in terms of solving matrix equations for the pressure field and the numerical treatment of the solid boundary. However, the general features of hydrodynamic phenomena are well simulated for both models, as indicated in the literature [46].

Results of the numerical computation of solitary wave transformation on a step ($h_1 = 10$ m, $h_2 = 5$ m, initial amplitude 0.3 m) within the framework of the Reynolds Averaged Navier–Stokes equations are displayed in Fig. 9. The difference between those two model results increases when the wave propagates over large distances. FLOW3D gives smaller wave amplitudes and speeds of propagation than CADMAS-SURF.

The main advantage of the Navier–Stokes equations is that they can describe the vertical structure of the velocity field. A snapshot of the vertical structure of particle velocities in the x–z plane is given in Fig. 10 (computing with FLOW3D). It is clearly seen that there is significant vertical motion of water particles in the vicinity of the step after the wave passes the step bathymetry (vertical and horizontal scales are not the same in Fig. 10). Due to viscosity, the weak "relict" let-like vertical motion on a step is visible after the waves are split into transmitted and reflected waves.

5. Discussion

First of all, the various model simulations will be compared for the reflected wave.

5.1. Transformation of reflected wave

The transformation of reflected waves computed in the framework of all models is shown in Figs. 11–13 for various distances from a step. Here the solid line corresponds to the EB-FEM model, the solid line with rhombs to the MIKE21 model, the solid line with points to the KdV model, the dashed line to the CADMAS model, and the solid line with crests to the FLOW3D model. These representations apply to all figures discussed below. Near the step (Fig. 11), wave shapes are almost the same for all numerical models. As distance from the step increases, the FLOW3D model predicts the delay in travel time of the reflected wave (Figs. 12 and 13). Meanwhile, all models give the same values for wave amplitudes. It is important to mention that due to the small wave amplitude, the soliton does not form at these distances.

5.2. Transformation of transmitted wave

The shapes of all modeled waves just after transformation on the step ($x = 4000$ m) are shown in Fig. 14. At the step, the waves modeled with the CADMAS and KdV models have almost the same shapes and amplitudes. Slightly smaller amplitudes are obtained in the other models. Perhaps this effect is related to the numerical smoothing of the bottom step in the Boussinesq-like models and to the wave dissipation in FLOW3D.

Fig. 15 shows wave shapes at the point 6400 m (2400 m from the step). The two secondary solitons are almost formed at this point. The predicted number of secondary solitons in the framework of the Korteweg–de Vries equation for $h_2/h_1 = 0.5$ is 3. The third soliton should have a very small amplitude, and it cannot be formed at this distance. Thus, this soliton is not present in Figs. 15 and 16. The amplitudes of the leading waves are almost the same in the CADMAS and KdV computations; the Boussinesq models give smaller amplitudes, and minimal amplitude is obtained in the FLOW3D computing. Nevertheless, the maximal difference in amplitudes is less than 5%.

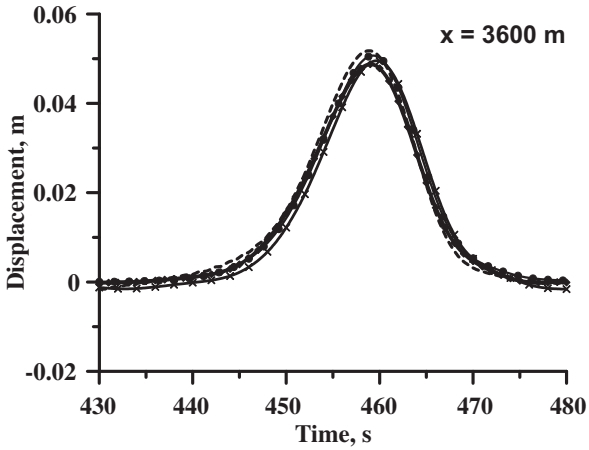


Fig. 11. Wave shapes at 400 m before the step. The solid line represents the EB-FEM model, the solid line with rhombs represents the MIKE21 model, the solid line with points represents the KdV model, the dashed line represents the CADMAS model and the line with crests represents the FLOW3D model.

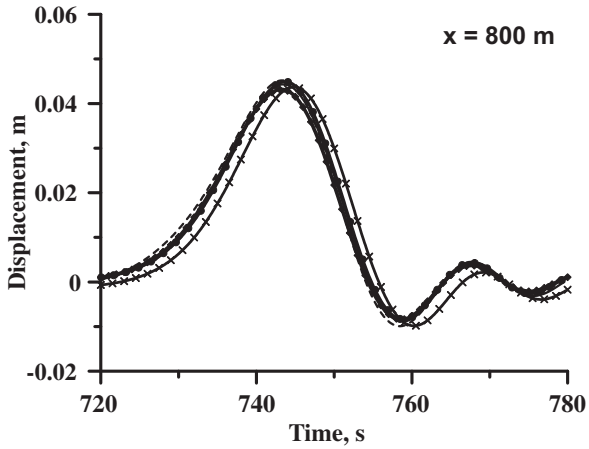


Fig. 12. Wave shapes at 3200 m before the step. The solid line represents the EB-FEM model, the solid line with rhombs represents the MIKE21 model, the solid line with points represents the KdV model, the dashed line represents the CADMAS model and the line with crests represents the FLOW3D model.

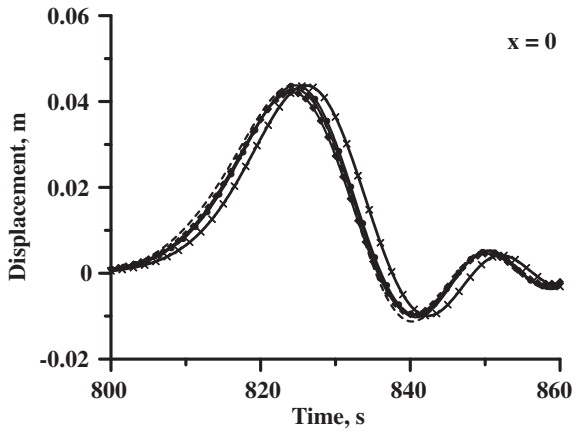


Fig. 13. Wave shapes at 4000 m before the step. The solid line represents the EB-FEM model, the solid line with rhombs represents the MIKE21 model, the solid line with points represents the KdV model, the dashed line represents the CADMAS model and the line with crests represents the FLOW3D model.

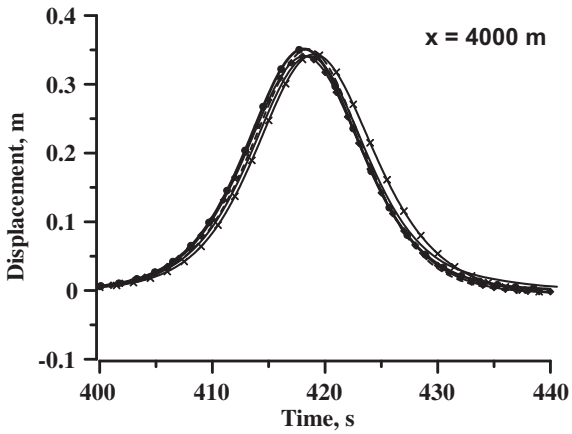


Fig. 14. Wave shapes on the step. The solid line represents the EB-FEM model, the solid line with rhombs represents the MIKE21 model, the solid line with points represents the KdV model, the dashed line represents the CADMAS model and the line with crests represents the FLOW3D model.

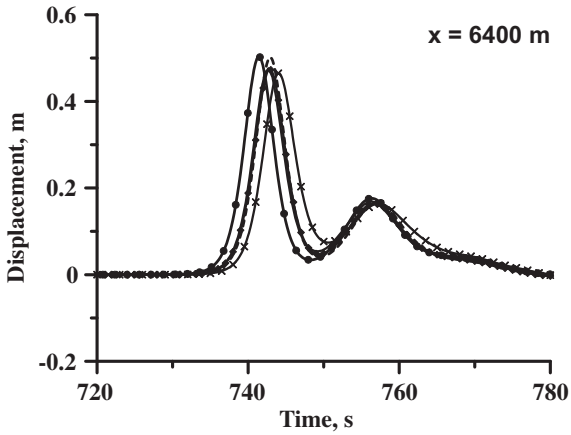


Fig. 15. Wave shapes at 2400 m after the step. The solid line represents the EB-FEM model, the solid line with rhombs represents the MIKE21 model, the solid line with points represents the KdV model, the dashed line represents the CADMAS model and the line with crests represents the FLOW3D model.

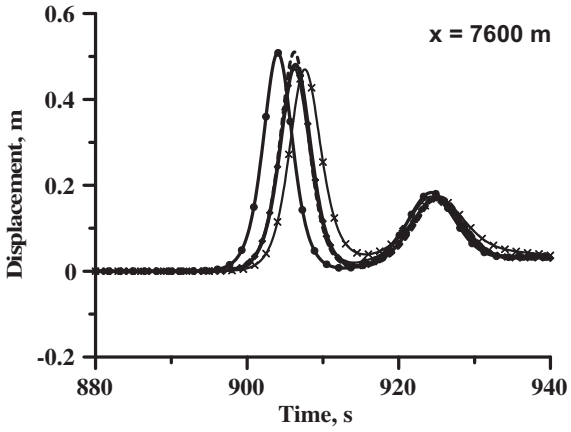


Fig. 16. Wave shape at 3600 m after the step. The solid line represents the EB-FEM model, the solid line with rhombs represents the MIKE21 model, the solid line with points represents the KdV model, the dashed line represents the CADMAS model and the line with crests represents the FLOW3D model.

There is more difference in the locations of the first (leading) wave within various models (Fig. 15) due to different speeds of soliton propagation. In the exact theory of water waves, the soliton speed decreases with amplitude (see, for instance, [48,49]), and this is why the KdV soliton derived in a weakly nonlinear limit has the maximal speed. Minimal speed is observed in FLOW3D computations, perhaps due to dissipative effects.

Fig. 16 displays the wave at distance 3600 m after a step (x = 7600 m). The leading soliton is fully formed and separated from the second wave. The amplitudes of the first soliton are 0.51 m for the KdV and CADMAS models, which coincides with the theoretically predicted value for the ratio $h_2/h_1 = 0.5$ and $H_0 = 0.3$ m. With increase of distance, the difference between the first soliton locations is increased; see Fig. 16. Meanwhile, the soliton speeds are almost the same in CADMAS and Boussinesq-like models, and differ from those in other models.

The second soliton is not finally formed at this distance, but due to its small amplitude there is no difference in amplitudes and locations across all models. Its amplitude at the point x = 7600 m (3600 m after step) is 0.18 m, which is very close to the predicted value 0.19 m in weakly nonlinear-dispersive theory.

Several computations are performed with different bottom steps, especially in the vicinity of the bottom step. The ratio h_2/h_1 in these runs is changed from 0.4 to 0.2. Computations are given with the FLOW3D code. The results of computing the wave passage through a step are compared with the predictions of the linear shallow-water theory; see Fig. 17. With decreasing depth ratio h_2/h_1 the computed wave amplitude is slightly smaller than predicted by the linear shallow-water theory, but the difference in amplitudes is less than 5%.

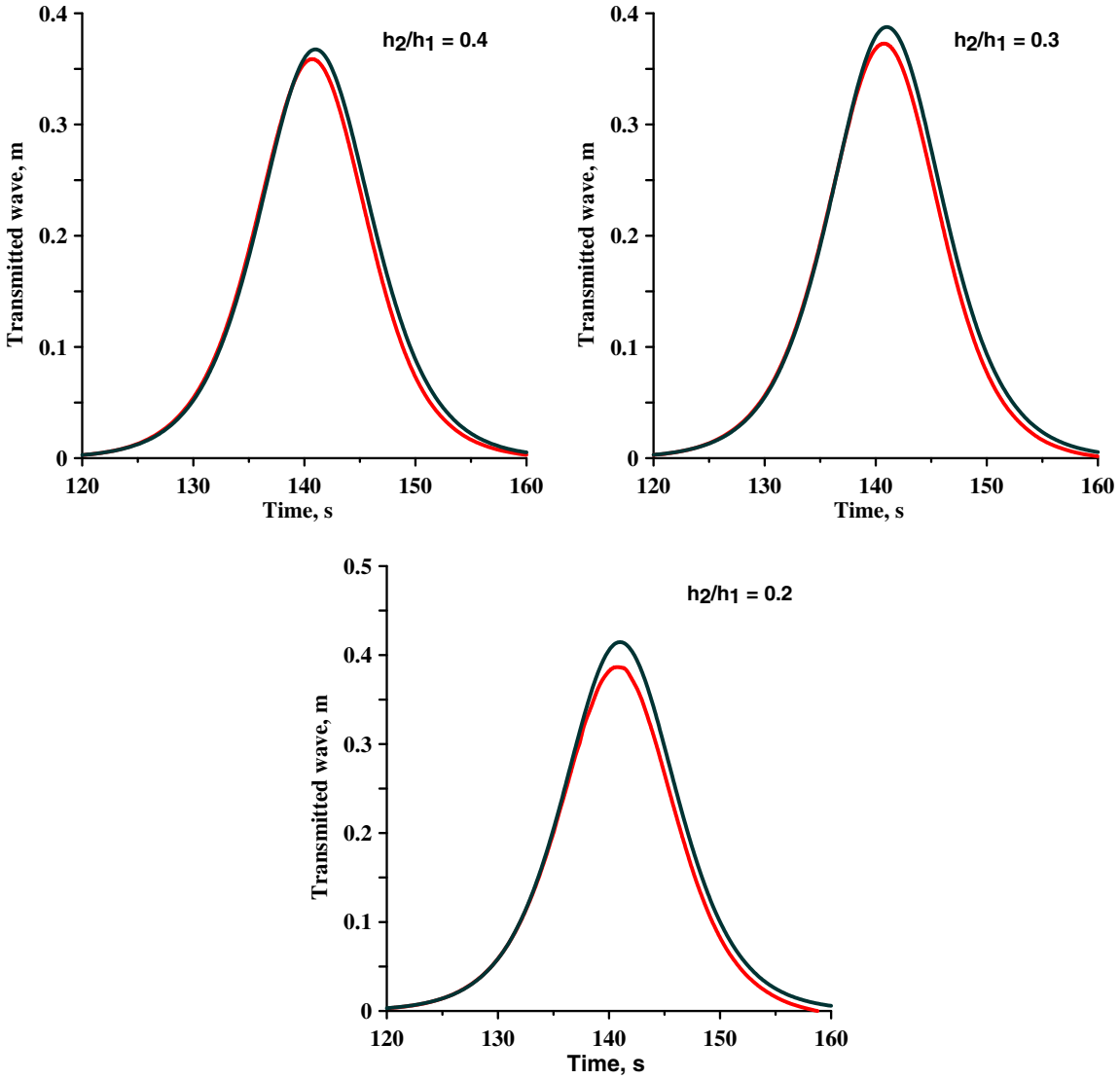


Fig. 17. Comparison of the theoretical transmitted wave shape (black line) and the wave shape as modeled in FLOW3D (grey line) for various ratios h_2/h_1.

6. Conclusion

A complex study of soliton transformation at the bottom step has been completed; it includes both analytical and computational parts. The weakly nonlinear-dispersive theory based on the Korteweg–de Vries equation is applied to study soliton fission in the wave field above the underwater step. Wave transformation on a step can be described in the framework of the linear shallow-water theory due to the weak amplitude of the solitary wave. Far from the step, nonlinear and dispersive effects become important, and the rigorous solutions of the Korteweg–de Vries equation are used to describe the process of soliton fission. The number and amplitudes of the secondary solitons appearing in transmitted and reflected waves are defined for different ratios h_2/h_1. Numerical simulation of solitary wave transformation is performed within various models: the uni-directional Korteweg–de Vries equation, 1D Boussinesq-like systems, and 2D Reynolds Averaged Navier–Stokes equations, five numerical models in all. The last RANS model allows description of the vertical structure of the wave flow. The theoretical predictions and results of the numerical simulations are compared. It is shown that the linear shallow-water theory accurately describes the passage of the weak-amplitude solitary wave through a step with $h_2/h_1 = 0.2 - 0.5$. Amplitudes of solitons appearing in the reflected and transmitted waves are almost equal, and the difference is less than 5% for all models. Our results concerning the soliton amplitudes are in good agreement with the numerical results of other authors [21–24]. The difference in travel time is more significant, which was not pointed out in the early literature. In particular, the wave modeled by the Korteweg–de Vries equation is faster, and the wave modeled by the FLOW3D model is slower than other modeled waves.

It is worth commenting the physical reasons for applicability of different models used in our study. Formally, the Boussinesq-like systems cannot describe the wave transformation on an abrupt geometry as a step. But as it follows from the rigorous linear theory, the step induces the evanescent modes with characteristic horizontal scale less then the water depth (significantly less then soliton length), which appear for short time of the soliton-step transformation. Such evanescent modes do not transfer the wave energy and do not contribute in the far field. It is why the Boussinesq-like models which do not include the evanescent modes (really they are of sub-grid scale) work properly to describe the "propagated" wave field. Numerically in our study, the discretization process is made that the numerical error behaves as numerical viscosity damped the short-scale oscillations like the evanescent modes. This numerical viscosity plays a similar role to the eddy viscosity in the model such as FLOW3D and CADMAS. The RANS model results are dependent on the length and time scale where the viscosity is important. In case where the turbulent flow is generated (e.g., flow passing through a step geometry), the eddy viscosity is much larger than molecular viscosity. And model scale should be small enough to capture the eddy viscosity effect. This requires the time step and grid length at least one or two order of magnitude smaller than that of frictionless models such as EB-FEM and MIKE21. This viscosity damps effectively the short-scale oscillations affecting the local flow at the step but not the far field. The same effects are included in other numerical models [21–24], where similar conclusions have been done.

Acknowledgements

This work was partially supported by BK21 and the Korean Ministry of Land, Transport and Maritime Affairs and also by the grants of the Leverhulme Trust (UK), RFBR (08-05-00069, 08-05-91850-EI, 09-05-91222-CT, 09-05-90408).

References

[1] F.D. Tappert, N.J. Zabusky, Gradient-induced fission of solitons, Phys. Rev. Lett. 27 (1971) 1774–1776.
[2] E.N. Pelinovskii, The evolution of a solitary wave in a nonhomogeneous medium, J. Appl. Mech. Tech. Phys. 12 (1971) 853–858.
[3] R.S. Johnson, Some numerical solutions of a variable-coefficient Korteweg–de Vries equation (with applications to solitary wave development on a shelf), J. Fluid Mech. 54 (1972) 81–91.
[4] A.C. Newell, Solitons in Mathematics and Physics, SIAM, CBMS-NSF, vol. 48, 1985.
[5] V. Djordjevic, L. Redekopp, The fission and disintegration of internal solitary waves moving over two-dimensional topography, J. Phys. Ocean. 8 (1978) 1016–1024.
[6] K.R. Helfrich, W.K. Melville, On long nonlinear internal waves over slope-shelf topography, J. Fluid Mech. 167 (1986) 285–308.
[7] C. Knickerbocker, A.C. Newell, Internal solitary waves near a turning point, Phys. Lett. 75A (1980) 326–330.
[8] R. Grimshaw, E. Pelinovsky, T. Talipova, Solitary wave transformation due to a change in polarity, Stud. Appl. Math. 101 (1998) 357–388.
[9] R. Grimshaw, E. Pelinovsky, T. Talipova, Solitary wave transformation in a medium with sign-variable quadratic nonlinearity and cubic nonlinearity, Physica D 132 (1999) 40–62.
[10] R. Grimshaw, E. Pelinovsky, T. Talipova, Soliton dynamics in a strong periodic field: the Korteweg–de Vries framework, Phys. Lett. A 344 (2005) 203210.
[11] E. Pelinovsky, Yu. Stepanjants, Transformation of a magnetoacoustic soliton in two-layer plasma, Sov. Tech. Phys. 20 (1975) 109–110.
[12] J.P. Germain, Coefficients de réflexion et de transmission en eau peu profonde, Rozprawy Hydrotechniezne 46 (1984) (in French).
[13] O. Nakoulima, N. Zahibo, E. Pelinovsky, T. Talipova, A. Kurkin, Solitary wave dynamics in shallow water over periodic topography, Chaos 15 (2005) 037107.
[14] R. Grimshaw, E. Pelinovsky, T. Talipova, Fission of a weakly nonlinear interfacial solitary wave at a step, Geoph. Astroph. Fluid Dyn. 102 (2008) 179–194.
[15] K.R. Khusnutdinova, A.M. Samsonov, Fission of longitudinal strain solitary wave in a delaminated bar, Phys. Rev. E 77 (2008) 066603.
[16] V. Maderich, T. Talipova, R. Grimshaw, E. Pelinovsky, B.H. Choi, I. Brovchenko, K. Terletska, D.C. Kim, The transformation of an interfacial solitary wave of elevation at a bottom step, Nonlinear Process. Geophys. 16 (2009) 33–42.
[17] S.R. Massel, Hydrodynamics of the Coastal Zone, Elsevier, Amsterdam, 1989.
[18] L.F. Bartholomeusz, The reflection of long waves at a step, Proc. Camb. Philos. Soc. 54 (1958) 106.
[19] N.R. Mirchina, E.N. Pelinovsky, Nonlinear transformation of long waves at a bottom step, J. Korean Soc. Coastal Ocean Eng. 4 (1992) 161–167.

[20] N. Sugimoto, N. Nakajima, T. Kakutani, Edge-layer theory for shallow-water waves over a step-reflection and transmission of a soliton, J. Phys. Soc. Jpn. 56 (1987) 1717–1730.
[21] F.J. Seabra-Santos, D.P. Renouard, A.M. Temperville, Numerical and experimental study of the transformation of a solitary wave over a shelf or isolated obstacle, J. Fluid Mech. 176 (1987) 117–134.
[22] K-A. Chang, T-J. Hsu, P.L.-F. Liu, Vortex generation and evolution in water waves propagating over a submerged rectangular obstacle, Coastal Eng. 44 (2001) 13–36.
[23] P.L.-F. Liu, Y. Cheng, A numerical study of the evolution of a solitary wave over a shelf, Phys. Fluids 13 (6) (2001) 1660–1667.
[24] P. Lin, A numerical study of solitary wave interaction with rectangular obstacles, Coastal Eng. 51 (2004) 35–51.
[25] C.C. Mei, Applied Dynamics of Water Waves, Word Sci., Singapore, 1989.
[26] P.G. Drazin, R.S. Johnson, Solitons: An Introduction, Cambridge Univ. Press, Cambridge, 1993.
[27] N.J. Zabusky, C.J. Galvin, Shallow-water waves, the Korteweg–de Vries equation and solitons, J. Fluid Mech. 47 (1971) 811–824.
[28] E.N. Pelinovsky, Nonlinear Dynamics of Tsunami Waves, Applied Physics Institute Press, Nizhny Novgorod, 1982 (in Russian).
[29] M.W. Dingenmass, Water Wave Propagation over Uneven Bottom, World Sci., Singapore, 1996.
[30] N. Zahibo, E. Pelinovsky, T. Talipova, A. Kozelkov, A. Kurkin, Analytical and numerical study of nonlinear effects at tsunami modelling, Appl. Math. Comput. 174 (2) (2006) 795–809.
[31] J. Grue, E. Pelinovsky, D. Fructus, T. Talipova, C. Kharif, Formation of undular bores and solitary waves in the Strait of Malacca caused by the 26 December 2004 Indian Ocean tsunami, J. Geophys. Res. 113 (2008) C05008, doi:10.1029/2007JC004343.
[32] J.L. Hammack, A note on tsunamis: their generation and propagation in an ocean of uniform depth, J. Fluid Mech. 60 (1973) 769–799.
[33] J.G. Caputo, Yu. Stepanyants, Bore formation, evolution and disintegration into solitons in shallow inhomogeneous channels, Nonlinear Process. Geophys. 10 (2003) 407–424.
[34] Yu.A. Berezin, Modeling Nonlinear Wave Processes, VNU Science Press, Utrecht, 1987.
[35] D.H. Peregrine, Long waves on a beach, J. Fluid Mech. 27 (1967) 815–827.
[36] Y. Chen, P.L.-F. Liu, Modified Boussinesq equations and associated parabolic models for water wave propagation, J. Fluid Mech. 288 (1995) 351–381.
[37] G. Wei, J.T. Kirby, S.T. Grilli, R. Subramanya, A fully nonlinear Boussinesq model for free surface waves. Part 1: highly nonlinear unsteady waves, J. Fluid Mech. 294 (1995) 71–92.
[38] P.A. Madsen, H.A. Schaffer, Higher-order Boussinesq-type equations for surface gravity waves: derivation and analysis, Philos. Trans. R. Soc. Lond. A. 356 (1998) 3123–3184.
[39] Y. Agnon, P.A. Madsen, H.A. Schaffer, A new approach to high order Boussinesq models, J. Fluid Mech. 399 (1999) 319–333.
[40] P.A. Madsen, H.B. Bingham, H.A. Schaffer, Boussinesq-type formulations for fully nonlinear and extremely dispersive water waves: derivation and analysis, Proc. R. Soc. Lond. A. 459 (2003) 1075–1104.
[41] S.-B. Woo, P.L.-F. Liu, Finite-element model for modified Boussinesq equations. I: model development, J. Waterway, Port, Coastal, Ocean Eng. 130 (2004) 1–16.
[42] V. Yakhot, S.A. Orszag, Renormalization group analysis of turbulence. I. Basic theory, J. Scient. Comput. 1 (1986) 1–51.
[43] V. Yakhot, L.M. Smith, The renormalization group, the e-expansion and derivation of turbulence models, J. Scient. Comput. 7 (1992) 35–61.
[44] Flow Science. FLOW-3D User's Manual. vols. 1 and 2, 2002.
[45] CDIT, Research and Development of Numerical Wave Channel. Coastal Dev. Inst. Technol., CDIT Libr. 12, 296p, 2001 (in Japanese).
[46] B.H. Choi, D.C. Kim, E. Pelinovsky, S.B. Woo, Three-dimensional simulation of tsunami run-up around conical island, Coastal Eng. 54 (2007) 618–629.
[47] B.H. Choi, E. Pelinovsky, D.C. Kim, I. Didenkulova, S.B. Woo, Two- and three-dimensional computation of solitary wave runup on non-plane beach, Nonlinear Process. Geophys. 15 (3) (2008) 489–502.
[48] M.S. Longuet-Higgins, J. Fenton, On the mass, momentum, energy and circulation of a solitary wave, Proc. R. Soc. Lond. A 337 (1974) 1–13.
[49] E.N. Pelinovsky, T.G. Talipova, Change of height of the solitary wave of large amplitude in the beach zone, Marine Geod. 2 (1979) 313–321.